Precambrian Research 249 (2014) 88–99

Contents lists available at ScienceDirect

Precambrian Research

journal homepage: www.elsevier.com/locate/precamres

Pinning northeastern Australia to northwestern Laurentia in the Mesoproterozoic

K.P.R. Medig[a,*], D.J. Thorkelson[a,1], W.J. Davis[b,2], R.H. Rainbird[b,3], H.D. Gibson[a,4], E.C. Turner[c,5], D.D. Marshall[a,6]

[a] Department of Earth Sciences, Simon Fraser University, 8888 University Drive, Burnaby, BC, Canada V5A 1S6
[b] Geological Survey of Canada, Natural Resources Canada, 601 Booth St., Ottawa, ON, Canada K1A 0E8
[c] Department of Earth Sciences, Laurentian University, 935 Ramsey Lake Road, Sudbury, ON, Canada P3E 2C6

ARTICLE INFO

Article history:
Received 7 February 2014
Received in revised form 25 April 2014
Accepted 28 April 2014
Available online 9 May 2014

Keywords:
Yukon
Mesoproterozoic
Columbia
Nuna
Supercontinents
Geochronology

ABSTRACT

Two supercontinents have been proposed for the latter half of the Precambrian: Columbia (or Nuna) from ca. 1.9 to 1.3 Ga, and Rodinia from ca. 1.1 to 0.75 Ga. In both supercontinents, Laurentia and Australia are regarded as probable neighbours, although their relative positions are contentious. Here we use detrital zircons ages from unit PR1 of the lower Fifteenmile group in Yukon, Canada, to demonstrate that northeastern Australia and northwestern Laurentia were firmly connected in the Mesoproterozoic. The zircon ages define a near-unimodal population with a peak at 1499 ± 3 Ma, which lies in an interval of magmatic quiescence on Laurentia, known as the North American magmatic gap (NAMG), and abundant magmatism in Australia. Sediment compositions and textures suggest the sediment was derived from a proximal metaplutonic source. We suggest that the Williams and Naraku batholiths in the Mt. Isa inlier in northeastern Australia, with crystallization ages ranging from 1493 ± 8 Ma to 1508 ± 4 Ma, are the most probable sources of sediment for the PR1 basin. The plutons were exhumed between 1460 and 1420 Ma, and likely formed an active, eroding highland in the Australian part of Columbia. Sediment derived from these plutons was carried eastward by a short, direct river system and deposited into the PR1 marine basin. Formation of the PR1 basin coincides with the formation of the southern Cordilleran Belt-Purcell, Hess Canyon, and Trampas basins. These basins, formed on the western margin of Laurentia, also have detrital zircon populations that fall into the NAMG, suggesting that sediment was derived from a non-Laurentian westerly source. The PR1 basin is herein correlated with the Belt-Purcell, Hess Canyon, and Trampas basins to the south, and together these basins record the onset of Columbia breakup along the length of the western margin of Laurentia from as far north as Yukon to as far south as Arizona.

1. Introduction

Supercontinental configurations are proposed, disputed, and refined. Some of the proposed Precambrian supercontinents are Rodinia (1.1–0.75 Ga), Columbia (1.9–1.3 Ga), and Nunavutia (2.45–2.05 Ga; Torsvik, 2003; Evans and Mitchell, 2011; Pehrsson et al., 2013). The proposed supercontinent Columbia, which broadly coincides with Nena and Nuna, has undergone many iterations based on a range of geologic and paleomagnetic evidence (Rogers and Santosh, 2002; Meert, 2002, 2012; Sears and Price, 2002; Zhao et al., 2002; Hou et al., 2008; Evans and Mitchell, 2011). Rogers and Santosh (2002) proposed the first testable reconstruction of Columbia by incorporating all of the cratons and linking rift basins along the western margin of Laurentia to those in India. Using a paleomagnetic approach, Meert (2002) refined Rogers and Santosh's reconstruction by providing latitudinal constraints to the paleo-configuration. Sears and Price (2002) proposed an alternative reconstruction, placing Siberia adjacent to Laurentia's western margin. Zhao et al. (2002) proposed another configuration for Columbia by linking 2.1–1.8 Ga orogens and Archean cratons and connecting eastern Australia to Laurentia's western margin. Another reconstruction moved Australia away from Laurentia and,

* Corresponding author. Tel.: +1 778 231 2693.
E-mail addresses: kmedig@gmail.com (K.P.R. Medig), dthorkel@sfu.ca (D.J. Thorkelson), Bill.Davis@nrcan-rncan.gc.ca (W.J. Davis), Rob.Rainbird@NRCan-RNCan.gc.ca (R.H. Rainbird), hdgibson@sfu.ca (H.D. Gibson), eturner@laurentian.ca (E.C. Turner), marshall@sfu.ca (D.D. Marshall).
[1] Tel.: +1 778 782 5390.
[2] Tel.: +1 613 943 8780.
[3] Tel.: +1 613 943 2212.
[4] Tel.: +1 778 782 7057.
[5] Tel.: +1 705 675 1151.
[6] Tel.: +1 778 782 5474.

http://dx.doi.org/10.1016/j.precamres.2014.04.018
0301-9268/

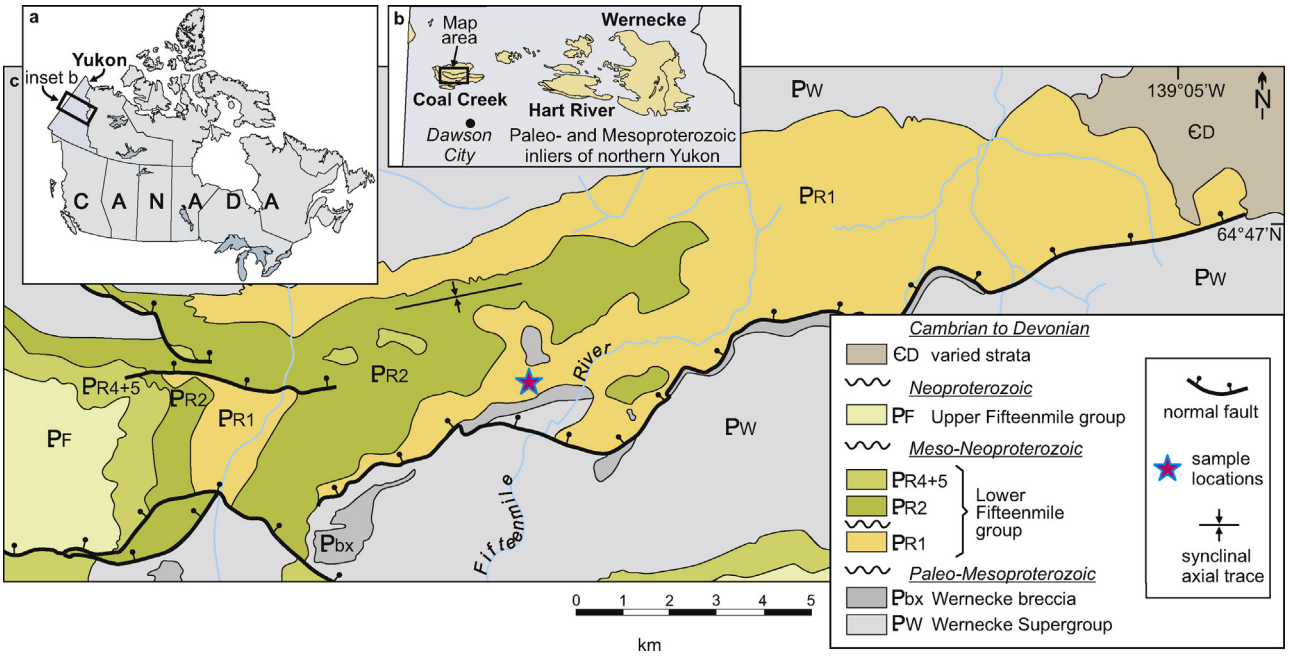

Fig. 1. Location and distribution of Proterozoic strata in the Coal Creek inlier, Western Ogilvie Mountains, Yukon, Canada (after Thompson et al., 1992). (a) Location of Proterozoic inliers (black rectangle) in Yukon, Canada. (b) Distribution of Paleo- and Mesoproterozoic inliers in northern Yukon. Map area highlighted by black rectangle north of Dawson City. (c) Paleoproterozoic to Devonian strata in the Coal Creek inlier. Samples were collected above the Wernecke Breccia near the base of unit PR1 (pink star). (For interpretation of the references to colour in this figure legend, the reader is referred to the web version of this article.)

based on a proposed radiating dyke swarm, placed North China along the margin of western Laurentia (Hou et al., 2008). Studies involving sedimentary provenance have generally favoured connections between western Laurentia, Australia and Antarctica (Ross and Villeneuve, 2003; Payne et al., 2009; Doe et al., 2012; Daniel et al., 2013).

The ongoing refinement of supercontinental configurations endures because most single pieces of evidence, and even groups of evidence, typically yield non-unique solutions that are open to debate (Buchan, 2013). In this study, we address the configuration of western Laurentia in the context of the supercontinent Columbia. Using new detrital zircon data from the lower Fifteenmile group unit PR1 in Yukon, Canada, we explore potential sediment source areas in Laurentia and on other continents, demonstrate a compelling new linkage between Australia and Laurentia, and provide a tightly constrained continental configuration for the early Mesoproterozoic.

2. Geologic setting and unit description

2.1. Regional geology

Unit PR1 is the lowest formation of the Meso-Neoproterozoic Fifteenmile group and is exposed in the Proterozoic Coal Creek inlier in the western Ogilvie Mountains of Yukon, Canada (Fig. 1). The Coal Creek inlier is one of three inliers of Proterozoic rocks exposed within the predominantly Phanerozoic cover in Yukon and is within the northwestern margin of the Cordilleran fold-thrust belt (Thompson et al., 1992). Proterozoic rocks in Yukon are exposed in contractional structures in successions that are as much as 22 km thick representing over 1 Ga of strata (Thorkelson et al., 2005). Crystalline basin rocks are nowhere exposed in Yukon and the age and composition of these rocks are not known (Thorkelson et al., 2005). The Coal Creek inlier is bound to the south by the north-verging Dawson Thrust which marks the boundary between the predominantly carbonate Paleoproterozoic to Ordovician strata of the Mackenzie platform to the north of the fault and finer clastic Neoproterozoic to Triassic strata of the Selwyn Basin to the south of the fault (Thompson et al., 1992; Rainbird et al., 1997). Unit PR1 unconformably overlies the regolith of the Paleoproterozoic Wernecke Supergroup (<1640 Ma) and zones of early Mesoproterozoic Wernecke Breccia (1599 Ma; Fig. 2 and Fig. 3a and b) (Thompson et al., 1992; Furlanetto et al., 2013). The underlying Wernecke Supergroup is comprised of two siliciclastic-to-carbonate grand cycles; including the Fairchild Lake Group, the Quartet Group and the Gillespie Lake Group, that have a cumulative minimum thickness of 14 km (Thorkelson et al., 2005). The Wernecke Supergroup underwent three phases of deformation, referred to as the Racklan Orogeny, prior to emplacement of the hydrothermal Wernecke

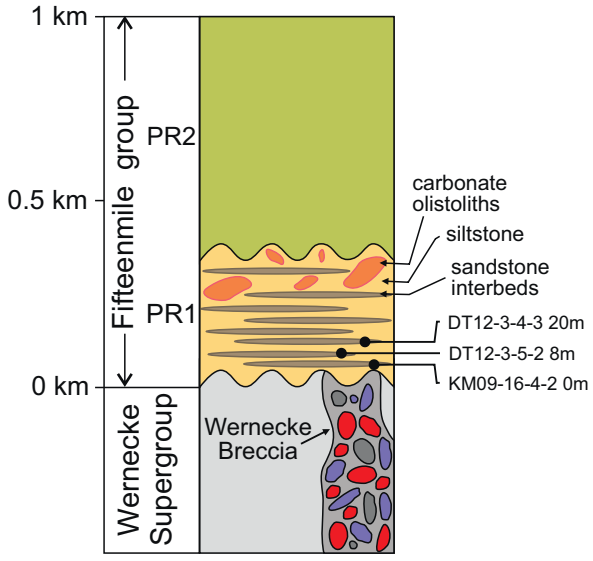

Fig. 2. Stratigraphic column of the Proterozoic Wernecke Supergroup and the lower Fifteenmile group in the Coal Creek inlier. Sample locations noted on right with height above the unconformity.

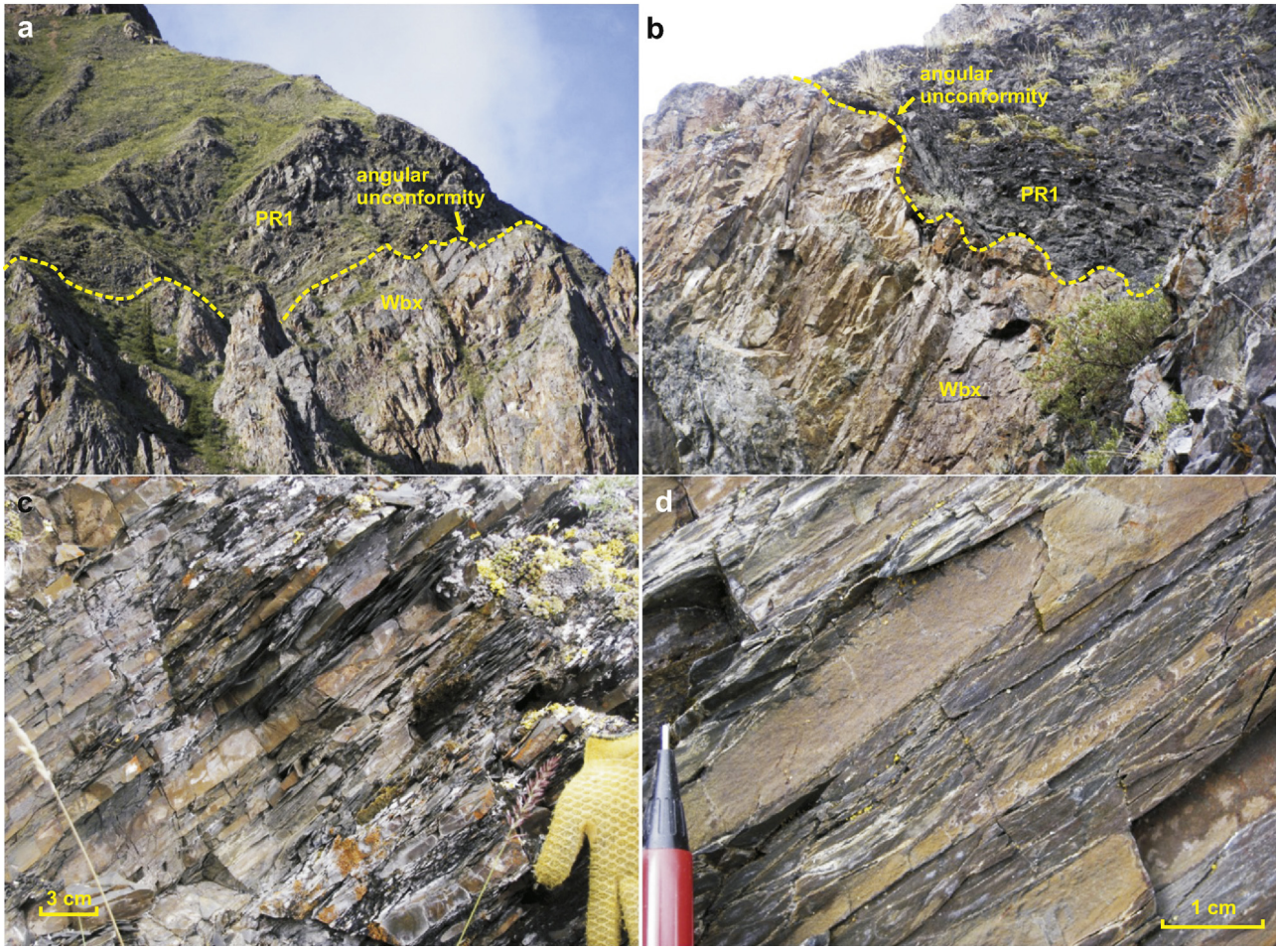

Fig. 3. Field relationships between the Wernecke Breccia and unit PR1. (a) and (b) Angular unconformity of regolith of orange–brown weathering Wernecke Breccia (Wbx) and dark grey unit PR1. (c) and (d) Unit PR1 turbidites of rusty brown weathering sandstone interbedded with dark grey siltstone. Samples were collected from sandstone interbeds similar to those displayed in the photo. (For interpretation of the references to colour in this figure legend, the reader is referred to the web version of this article.)

Breccia (Brideau et al., 2002; Thorkelson et al., 2005). Unit PR1 is unconformably overlain by unit PR2 of the lower Fifteenmile group and younger strata including units PR4 and PR5 of the lower Fifteenmile group and Paleozoic strata. Unit PR2 unconformably overlies unit PR1 in the eastern part of the inlier, but lies directly on the Wernecke Supergroup to the west. Unit PR2 is comprised of yellow to blue–grey weathering dolostone. Unit PR4 and PR5 are medium-grey dolomite breccia with uncommon stromatolitic dolostone and shale to pebbly mudstone, respectively (Thompson et al., 1992).

2.2. Unit PR1

Unit PR1 is approximately 320 m thick and consists of interbedded sandstone and mudstone with scattered carbonate olistoliths (Thompson et al., 1992). The olistoliths are orange to brown weathering and range in diameter from less than a metre to several metres. The strata are dominated by couplets of brown-weathering sandstone and dark grey to rusty-weathering siltstone (Fig. 3c and d). The sandstone is predominantly medium grey, moderately to well sorted, massive to laminated lithic wacke. The wacke is predominantly fine grained but varies from very fine grained to coarse grained, and forms beds 5–20 cm thick. The strata are interpreted as ABD Bouma division turbidites with intervening hemipelagic sediment. Olistoliths deposited in turbidite units in the upper portion of PR1 suggest that the basin was tectonically active. Paleocurrent indicators were not identified in the unit.

2.2.1. Petrography

Seven samples, including KM09-16-4-1, KM09-16-4-2, DT12-3-4-1, DT12-3-4-2, DT12-3-4-3, DT12-3-5-1, and DT12-3-5-2, were collected in the lower 20 m of unit PR1 above the regolith of Wernecke Breccia.

Fine-grained lithic wacke consists of angular to subrounded framework grains (85–90%) in a muddy matrix (10–15%). Framework grains include quartz (20–40%), muscovite, biotite, chlorite, feldspar (partially replaced by calcite), zircon, apatite, and perthite (collectively 10–20%) with the rest of the rock consisting of lithic clasts, including mudstone (40–60%; Fig. 4a–d). Muscovite (not shown) and biotite are oriented parallel to bedding. Biotite and chlorite grains are bent or kinked around more competent grains, such as quartz, probably due to compaction (Fig. 4a–c).

Coarse-grained lithic wacke consists of a framework (80–85%) of moderately to well-sorted, rounded to subrounded quartz grains and polycrystalline quartz with up to 80 subdomains (40–50%), carbonate (15%), feldspar (10%), and lithic grains (25–35%; Fig. 4e and f). Calcite, limonite, and quartz cement (15–20%) fill the void spaces and quartz cement is evident as quartz overgrowths on subrounded to subangular grains (Fig. 4e and f).

3. Methods

Three of the seven samples collected from the base of unit PR1 were processed for geochronological analysis at Simon Fraser University using standard crushing and milling techniques, with

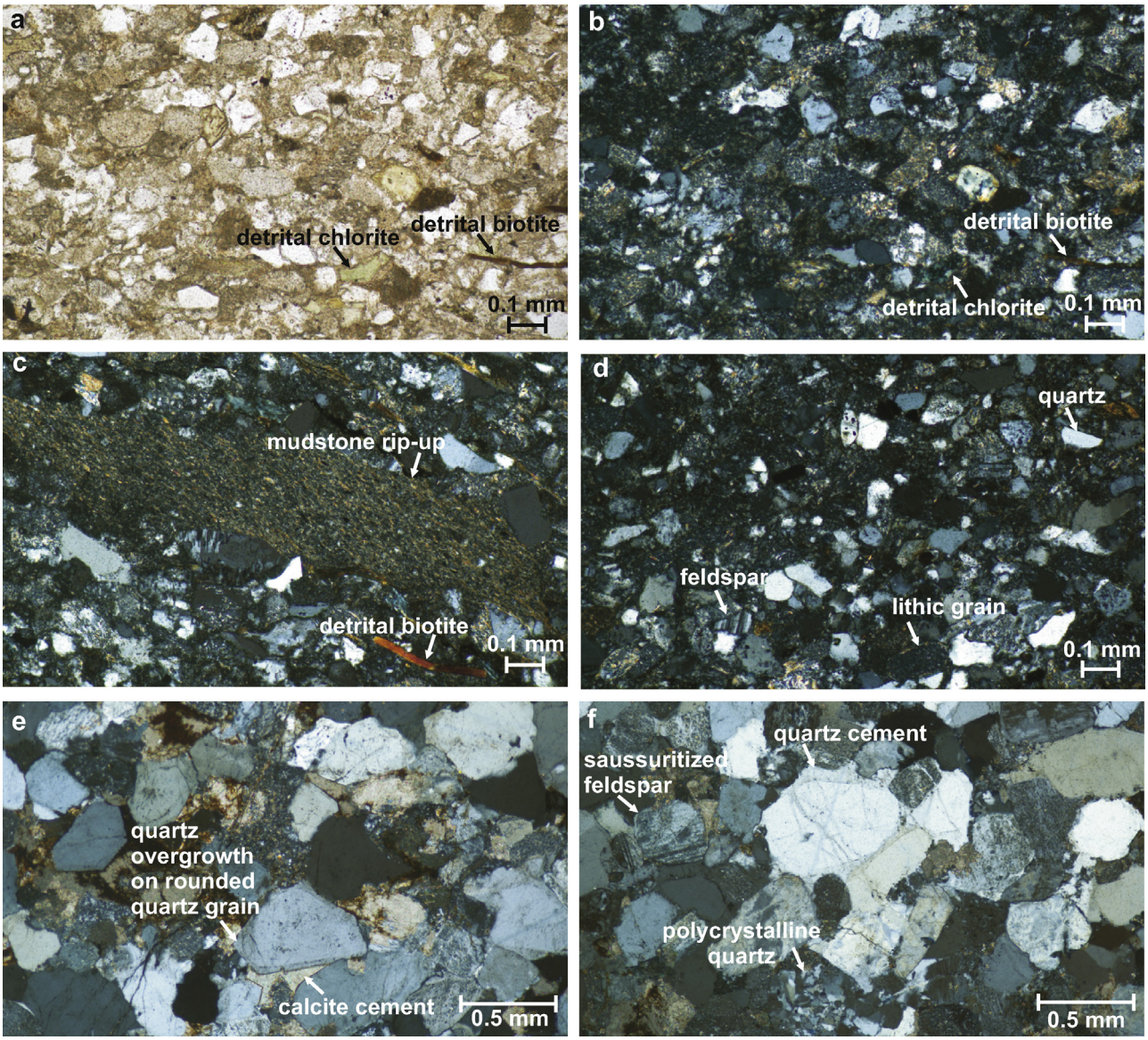

Fig. 4. (a) Thin section of brown-weathering, medium grey, very fine-grained lithic wacke (sample KM09-16-4-2). Planar-laminated sandstone with muddy matrix and clasts of angular to subangular quartz grains, lithic grains, detrital chlorite grains, and detrital biotite grains deformed during compaction; plane-polarized light (PPL). (b) Same as (a) in cross-polarized light (XPL). (c) Mudstone rip-up and kinked detrital biotite in sample KM09-16-4-2; XPL. (d) Thin section of sample DT12-3-4-3, brown-weathering, medium grey fine-grained lithic wacke overlying dark grey mudstone. XPL image of coarser fraction: fine-grained lithic wacke with angular feldspar, quartz, and subrounded lithic grains. (e) Thin section of sample DT12-3-5-2, brown-weathering, light grey, coarse-grained wacke. Quartz overgrowths on subrounded quartz grains, calcite interstitial cement; XPL. (f) Saussuritized feldspar, quartz cement, lithic grains, polycrystalline quartz in sample DT12-3-5-2; XPL. (For interpretation of the references to colour in this figure legend, the reader is referred to the web version of this article.)

mineral separation using a Wilfley table and heavy liquids. The first sample, KM09-16-4-2, was chosen to represent unit PR1 as part of a larger sample set from Proterozoic inliers across Yukon. After identifying a near-unimodal population in sample KM09-16-4-2, two additional samples were chosen from unit PR1 for geochronological analysis to confirm if the near-unimodal population identified in the first sample was reflective of the detrital zircon population in the unit and if the near-unimodal age was independent of grain-size and height above the unconformity. Analyses included one coarse-grained (DT12-3-5-2) and two fine-grained (KM09-16-4-2 and DT12-3-4-3) samples. The samples were collected directly above the contact with the underlying Wernecke Breccia (KM09-16-4-2), and 8 m (DT12-3-5-2) and 20 m (DT12-3-4-3) above the contact (Fig. 2).

Following sample processing, grains were examined for variability and it was noted that although there was variability in size, the morphology of the grains was remarkably consistent. To avoid biasing, detrital zircon grains were randomly chosen from the processed sample without preference to colour, shape, wholeness, or size. A statistically adequate number of grains were selected from unit PR1 to ensure that any fraction of a population representing more than 0.05 of the total population was included with a 95% confidence level (Vermeesch, 2004).

Grains were mounted on an epoxy puck, polished, and coated with gold at the J.C. Roddick Ion Microprobe Laboratory at the Geological Survey of Canada (GSC) in Ottawa. The mounted grains were imaged on a scanning electron microscope (SEM) at the GSC using both back-scattered electron (BSE) and cathodoluminescent (CL) imaging techniques.

The samples were analysed in two different sessions on the sensitive high resolution ion microprobe (SHRIMP II) at the GSC in Ottawa following analytical procedures outlined by Stern (1997).

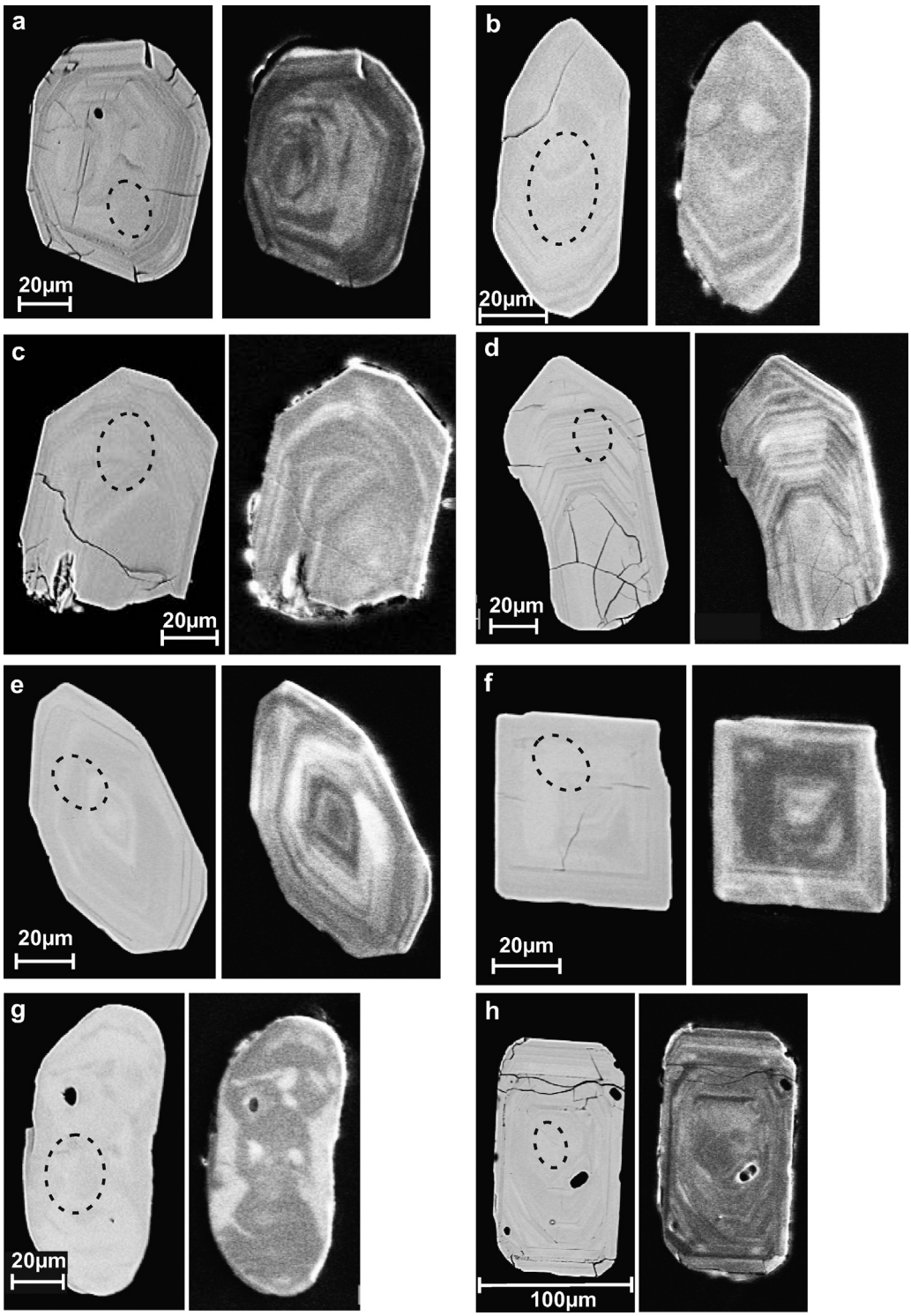

Fig. 5. SEM back-scattered electron (BSE) and cathodoluminescent (CL) images of representative zircon grains from the samples analysed. Dashed black circles represent approximate location of SHRIMP spots. (a) Zircon grains from sample KM09-16-4-2. SEM BSE image (left) and CL image (right) of grain 10704-21.1 with partially rounded corners, radial fracturing from the grain boundary, oscillatory zoning within the grain, and an inclusion in the northwest quadrant (black circle <5 μm). (b) Equant and oscillatory zoned zircon grain 10704-6.1 BSE (left) and CL (right) images (sample KM09-16-4-2). (c) BSE (left) and CL (right) images of oscillatory zoned, euhedral, broken zircon grain 10704-3.1 (sample KM09-16-4-2). (d) Sample DT12-3-4-3 BSE (left) and CL (right) images of oscillatory zoned zircon grain 10908-4.1 with fractured core. (e) Equant, euhedral, and oscillatory grained zircon 10908-27.1 with no fractures. BSE (left) and CL (right) images (sample DT12-3-4-3). (f) BSE (left) and CL (right) images of rhomboidal zircon grain 10908-79.1 with oscillatory zoning (sample DT12-3-4-3). (g) Sample KM09-16-4-2 BSE (left) and CL (right) images of Archean zircon grain 10704-5.1 with well-rounded corners and a lack of oscillatory zoning. (h) BSE (right) and CL (right) images of equant zircon grain 10909-36.1 with multiple inclusions (sample DT12-3-5-2).

Sample KM09-16-4-2 (GSC mount No. IP639) was analysed in the first session with a primary ion beam Kohler aperture of 120 μm resulting in a 17 × 23 μm spot size. The second session included samples DT12-3-4-3 and DT12-3-5-2 (GSC mount No. IP662), and used a primary ion beam Kohler aperture of 100 μm resulting in a spot size of 13.5 × 19 μm. Spot sizes were selected based on the size of crystals and the available target areas. Pb/U calibration was based on Sri Lankan zircon standard z6266 with an accepted age

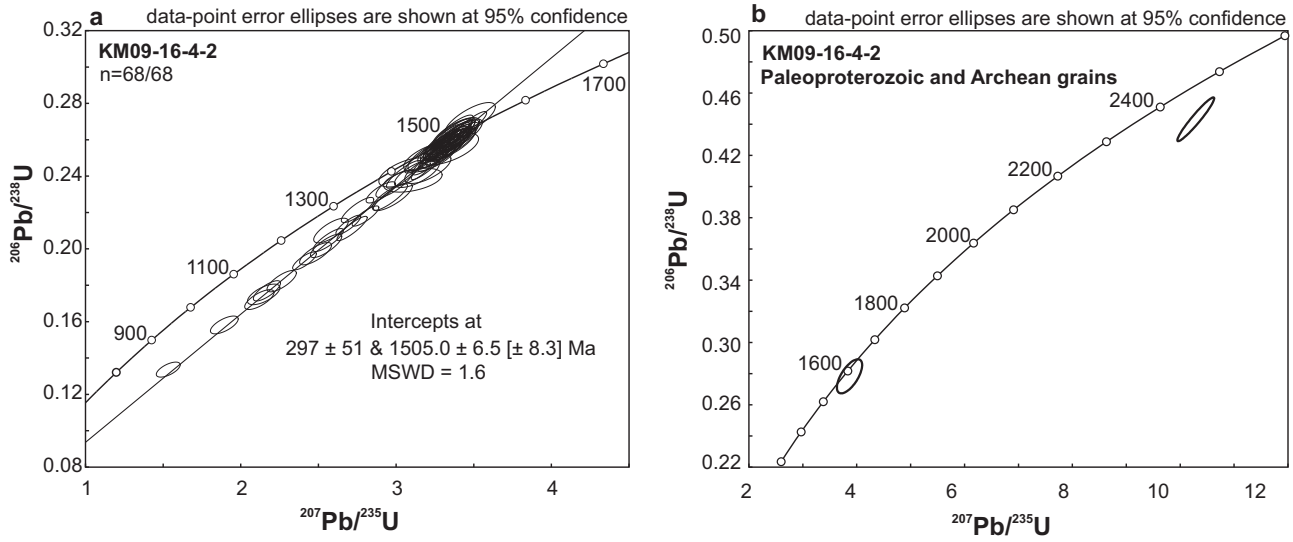

Fig. 6. Concordia plot of sample KM09-16-4-2 (n = 68/68). (a) An upper intercept age of 1505.0 ± 6.5 Ma was determined from 68 grains. The lower intercept of the chord results in an age of 297 ± 51 Ma and reflects an event resulting in lead loss. (b) The sample included one Paleoproterozoic and one Archean grain that did not fall into the Mesoproterozoic near-unimodal population shown in (a).

of 559.0 ± 0.2 Ma (Stern and Amelin, 2003). Internal GSC zircon standard z1242, with an age of 2679.7 ± 0.3 Ma, was used to monitor accuracy of the measured $^{207}Pb/^{206}Pb$ ratio. Data was compiled using Squid-2 software (Ludwig, 2009) and analysed with Isoplot 3.75 (Ludwig, 2012).

4. Results

4.1. Geochronology

Three of the seven samples collected were analysed for U–Pb isotopic ratios including KM09-16-4-2, DT12-3-4-3, and DT12-3-5-2. Detrital zircon grains (ca. 1500 Ma) extracted from the three samples display prismatic form with moderately to slightly rounded terminations, oscillatory zoning, and are from 25 to 200 μm long (Fig. 5a–f, and h). Some grains are devoid of fractures (e.g. Fig. 5e) and others display fractures both in the core and on the perimeter of the grain (e.g. Fig. 5d). Some grains have small (5–10 μm) inclusions (e.g. Fig. 5a, g, and h). Fractures are primary features of the zircon grains. In contrast to the ca. 1500 Ma grains, the Paleoproterozoic and Archean grains have well-rounded terminations and lack oscillatory zoning (e.g. Fig. 5g).

A total of 167 representative zircon grains from 3 samples were analysed for U and Pb isotopes using a sensitive high-resolution ion microprobe (SHRIMP II; see inline supplementary Table 1). A total of 72 analyses were completed on 70 zircon grains from sample KM09-16-4-2. Two analyses were duplicate analyses from the same grain and were not included in the age calculation. Sixty-eight of the 70 grains lie on a discordia line with an upper intercept age of 1505 ± 6.5 Ma along with one Neoarchean (2543 ± 7 Ma) grain and one Paleoproterozoic (1647 ± 34 Ma) grain (Fig. 6). Data-point error ellipses are shown at 95% confidence. The discordant data reflect Pb-loss and produce a lower chord intercept of 297 ± 51 Ma.

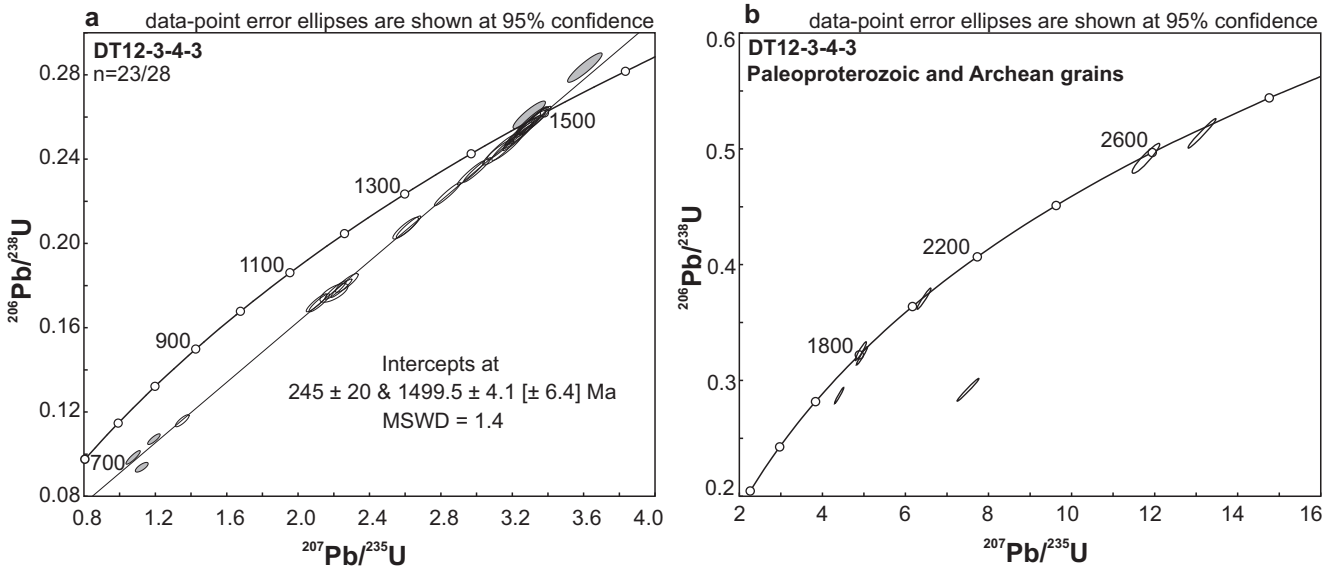

Fig. 7. Concordia plot of sample DT12-3-4-3 (n = 23/28). (a) Five analyses (shaded in grey) were not included in the age calculation because they did not fall directly on the chord. An upper intercept age of 1499.5 ± 4.1 Ma was determined from 23 grains. The lower intercept age is 245 ± 20 Ma. (b) Seven Proterozoic and Archean grains not included in (a).

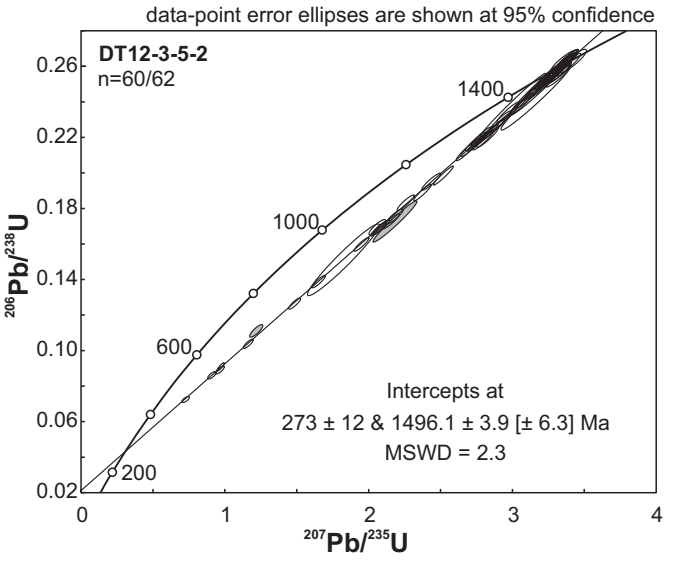

Fig. 8. Concordia plot of sample DT12-3-5-2 (n = 60/62). Two analyses (shaded in grey) were not included in the age calculation because they did not fall directly on the chord. Upper intercept age of 1496.1 ± 3.9 Ma determined from 60 grains. A lower intercept age of 273 ± 12 Ma indicates an event resulting in lead loss occurred at this time.

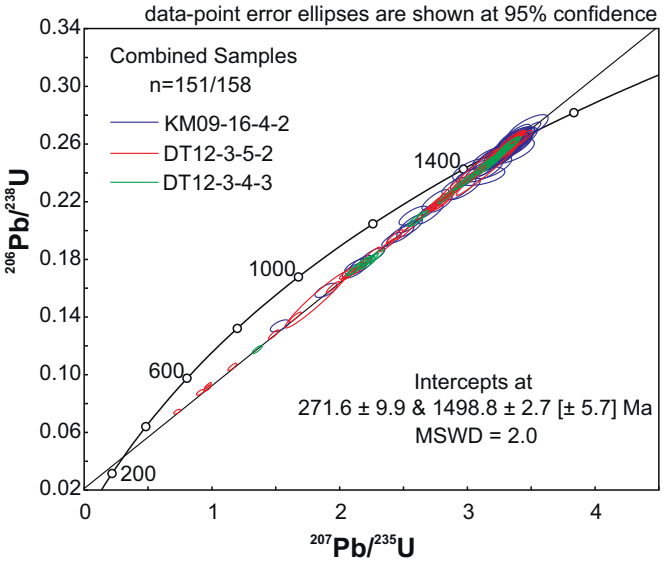

Fig. 9. Combined U–Pb data from samples KM09-16-4-2 (blue), DT12-3-4-3 (green), and DT12-3-5-2 (red). Given precision for individual analyses and the degree of scatter (MSWD = 2.0), the age of the main source area represents ages ranging from slightly younger to slightly older than the upper intercept age of ca. 1500 Ma. Data point error ellipses are shown at 95% confidence. Proterozoic and Archean grains are not displayed. (For interpretation of the references to colour in this figure legend, the reader is referred to the web version of this article.)

A total of 37 analyses were completed on 35 grains from sample DT12-3-4-3. Two analyses represent duplicate analyses on the same grain and were not included in the age calculation. In addition, five grains were not included in the age calculation because they did not fall on the chord and reflect either lead loss or uranium gain differing from the collective suite of analyses. Twenty-three grains lie on a discordia line with an upper intercept age of 1499.5 ± 4.1 Ma (Fig. 7a). The lower intercept of the chord reflects lead loss at approximately 245 ± 20 Ma. The remaining zircon grains include three Neoarchean (2734 ± 4 Ma, 2717 ± 4 Ma and 2610 ± 7 Ma) and four Paleoproterozoic (2065 ± 5 Ma, 1850 ± 6 Ma, 1846 ± 5 Ma, and 1817 ± 7 Ma) grains (Fig. 7b).

Sixty-four analyses, including two duplicate analyses, were completed on 62 grains from sample DT12-3-5-2. Two analyses were not included in the age calculation because they did not follow the trajectory of lead loss of the other 60 analyses. Collectively, the remaining 60 analyses lie on a discordia line with an upper intercept age of 1496.1 ± 3.9 Ma with Pb-loss at 273 ± 12 Ma (Fig. 8). Older grains were not identified in the sample.

The combined one hundred and fifty-one analyses from the three individual samples define a chord on a concordia diagram with an upper intercept age of 1498.8 ± 2.7 Ma (MSWD = 2.0, n = 151/158) and lower intercept of 271.6 ± 9.9 Ma (Fig. 9). Of the 16 grains not included in the upper intercept age determination, 7 grains were discarded because they plot away from the chord and have uncertain ages. The remaining 9 grains have Paleoproterozoic (2065 ± 5 to 1647 ± 34 Ma) and Neoarchean (2734 ± 4 to 2543 ± 7 Ma) ages (see inline supplementary Table 1). Given the precision for individual analyses and the degree of scatter (MSWD = 2.0), the population of grains probably reflects a limited range of ages within a few million years of 1500 Ma rather than a single age at 1498.8 Ma.

5. Discussion

5.1. Sediment provenance

A dominant and narrow peak in a population of detrital zircon ages is commonly attributed to a horizon of air-fall tuff (e.g. Macdonald et al., 2010; Daniel et al., 2013). In such cases, the age of the peak would date both the age of volcanism and sedimentation. The zircon grains would tend to be euhedral with sharp, angular terminations, and the host sediment would typically contain tuffaceous components such as glass shards (or their devitrified remnants), angular rock and mineral grains, and embayed quartz grains. Although the zircon data from unit PR1 does display a near-unimodal age population with a pronounced peak at 1498.8 ± 2.7 Ma, neither euhedral zircon nor tuffaceous components are present in the sandstone from unit PR1. Instead, the zircon grains have moderately to slightly rounded terminations, and the shapes of the other mineral grains range from subangular to subrounded.

The detrital mineral assemblage of unit PR1 is consistent with derivation from a weakly metamorphosed plutonic source rather than a *syn*-sedimentary volcanic eruption. The assemblage includes polycrystalline quartz, perthite, plagioclase, carbonate, chlorite, biotite, detrital chlorite, oscillatory-zoned zircon, and large quartz grains (>0.5 mm) (Figs. 4 and 5). The quartz–perthite–plagioclase–biotite–zircon assemblage is consistent with a granitic source, but detrital chlorite, as well as a strained and polycrystalline texture of some of the quartz, implies that the granitoid source had undergone weak metamorphism and deformation. Additional grain types include mudstone and fine-grained lithic clasts, some of which were deformed during compaction and suggest that the source area also included unconsolidated sediment that was penecontemporaneous with the PR1 basin.

Immature sedimentary textures, including minimal rounding and sorting, and a near-unimodal detrital zircon population indicate limited transport of sediment from a nearby and areally restricted source. We postulate that detritus was derived almost exclusively from a nearby granitic highland and was transported in a short, direct river system probably less than 2 km (cf. Cawood et al., 2003; Sláma and Košler, 2012) into the PR1 basin, where it was re-deposited into deeper water by gravity flows. There is no evidence for a local 1500 Ma granitic highland in Yukon that could have served as a proximal source for sediment for the PR1 basin.

Metaplutonic source rocks ca. 1500 Ma in age are rare in Laurentia. This age lies within the North American magmatic gap (NAMG; Ross and Villeneuve, 2003), an interval of minimal igneous activity in western Laurentia, which extends from 1610 to 1490 Ma. The few known NAMG events in Laurentia can be precluded as sources for the PR1 basin. Specifically, the 1540 Ma Kuungmi volcanics in the Thelon Basin, northern Canada, the 1577 Ma Laclede augen gneiss of the Priest River complex in northern Idaho, USA, and the 1590 Ma Western Channel diabase near eastern Great Bear Lake, Northwest Territories, Canada are too old (Doughty et al., 1998; Hamilton and Buchan, 2010; Chamberlain et al., 2010). The ca. 1500 Ma granitoid rocks in the Pinware terrane of eastern Canada (Heaman et al., 2004) are the correct age, but are too distant to be considered a source.

The unsuitability of Laurentia as a sediment source for the PR1 turbidites implies that the sediment was likely derived from another continent. Even on a global scale, however, igneous sources of ca. 1500 Ma are limited (Condie et al., 2009). Some ca. 1500 Ma igneous events are present in São Francisco Craton, Siberia, and Congo (Condie et al., 2009; Ernst et al., 2013; Silveira et al., 2013; Pisarevsky et al., 2014). These events include the Curaçá dyke swarm and the Chapada Diamantina dykes and sills on the São Francisco Craton dated at 1506.7 ± 6.9 Ma and 1501.0 ± 9.1 Ma, respectively (Silveira et al., 2013); the Humpata dolerite sills dated at 1501.5 ± 3.6 Ma that intrude the volcano-sedimentary sequence of the Chela Group on the Congo Craton (Ernst et al., 2013); and the Kuonamka dykes in the Anabar Shield with U–Pb ages of 1503 ± 5 Ma in Siberia (Ernst et al., 2000). Although these events reflect ca. 1500 Ma events, they are not suitable source rocks for the PR1 basin because they are primarily igneous events dominated by mafic rocks, rather than granitic rocks. In addition, paleomagnetic constraints on reconstructions show that these continents were not adjacent to the western margin of Laurentia in the Mesoproterozoic (Pesonen et al., 2012; Pisarevsky et al., 2014). Instead, both the Congo and São Francisco cratons were well north of Laurentia (present day coordinates) between 1500 and 1450 Ma (Pisarevsky et al., 2014). Siberia was west of Congo and to the northwest of Laurentia (present day coordinates) ca. 1500 Ma (Pisarevsky et al., 2014).

Abundant sources for NAMG-aged zircon grains have been identified in eastern Australia and northern and eastern Antarctica (Ross et al., 1992; Page and Sun, 1998; Peucat et al., 2002; Ross and Villeneuve, 2003; Betts et al., 2009; Goodge et al., 2010). As much of Antarctica is covered in ice, NAMG-aged sources consist of clasts found in till with local provenance inferred to be beneath the ice. In northern Antarctica, a clast derived from felsic volcanics within the Terre Adélie Craton was dated at 1595 ± 9 Ma (Peucat et al., 2002). The Terre Adélie Craton, located on the northern tip of Antarctica, was formerly a portion of the Mawson Continent that also included the Gawler Craton of south Australia (Payne et al., 2009). At this time, the Gawler Craton was amalgamated with the west and north Australian cratons (Betts and Giles, 2006). On the eastern coast of Antarctica, in the Transantarctic Mountains, another NAMG-age was identified in a granite clast from a moraine near the Lonewolf Nunataks with a zircon U–Pb age of 1578.0 ± 5.2 Ma (Goodge et al., 2010). Although these ages fall into the NAMG, all of the ages from Antarctica are too old to be plausible sources for detritus in the PR1 basin.

In Australia, sediment sources span the full range of the NAMG from approximately 1600 to 1490 Ma and include possible ca. 1500 Ma sources. NAMG sources are located in the Gawler Craton (1615 ± 8 to 1574 ± 5 Ma), the Georgetown inlier (1554 ± 10 to 1544 ± 7 Ma), the Curnamona Province (1590 to 1579 ± 1.5 Ma), the Musgrave Province/Arunta inlier (1590 ± 25 to 1557 ± 24 Ma), and, most relevant to the PR1 basin, the Mount Isa inlier (1547 ± 5 to 1493 ± 8 Ma; Ross et al., 1992; Page and Sun, 1998; Ross and Villeneuve, 2003; Betts et al., 2009). Importantly, reliable paleomagnetic data support the proximity of Australia to Laurentia between 1650 and 1380 Ma (Pesonen et al., 2012; Pisarevsky et al., 2014). Consequently, we explore the remaining provenance option, Australia, using geochronology, petrology and structural geology.

5.2. Constraints on Australia–Laurentia linkage

Late Paleoproterozoic to early Mesoproterozoic deformation is preserved in rocks from western Laurentia (Thorkelson et al., 2005; Duebendorfer et al., 2006). In the northern Cordillera, the Racklan orogeny (1640–1599 Ma; Thorkelson et al., 2005; Furlanetto et al., 2013) produced three phases of deformation and greenschist facies metamorphism in the Wernecke Supergroup (Thorkelson et al., 2005). The latter phase of the Racklan orogeny involved the obduction of a volcanic–plutonic nappe, termed Bonnetia, onto the western margin of Laurentia (Furlanetto et al., 2013; Nielsen et al., 2013). Bonnetia may have been an island arc or the leading edge of another continent (Furlanetto et al., 2013; Nielsen et al., 2013). The Racklan orogeny is broadly synchronous with thick-skinned deformation of the Forward orogeny in the western Northwest Territories of Canada (MacLean and Cook, 2004). In southwestern Laurentia, concurrent deformation is recorded by contractional structures in the Cheyenne belt in southern Wyoming (Duebendorfer et al., 2006). In the southern Sierra Madre, $^{40}Ar/^{39}Ar$ dates between 1620 and 1590 Ma record a thermal and deformational event indicating reactivation along an Archean–Proterozoic suture (Duebendorfer et al., 2006). Collectively, these events record deformation along the western margin of Laurentia that was contemporaneous with collision of juvenile island arcs with southern Laurentia during the Mazatzal orogeny (Karlstrom et al., 2001; Furlanetto et al., 2013).

In northeastern Australia, the Isan orogeny occurred from ca. 1620 to 1500 Ma and has been suggested as a possible correlative of the Racklan orogeny (Thorkelson et al., 2005). The second phase of the Isan orogeny (1540–1500 Ma) records east–west shortening in the Mount Isa inlier and granitic plutonism from 1547 ± 5 Ma to 1493 ± 8 Ma, and has been proposed as the event that brought Australia and Laurentia together (Page and Sun, 1998; Betts et al., 2008, 2009). Components of the Williams and Naraku batholiths in the Eastern Fold Belt of the Mount Isa inlier have ages that are indistinguishable from the detrital zircon ages from the PR1 basin. In particular, the Wimberu granite (1508 ± 4 Ma), the Malakoff granite (1505 ± 5 Ma), the Capsize granodiorite (1501 ± 6 Ma), and the Yellow Waterhole granite (1493 ± 8 Ma; Page and Sun, 1998). Cooling histories based on ^{40}Ar–^{39}Ar hornblende and biotite dates indicate that the batholiths were exhumed between 1460 and 1420 Ma (Spikings et al., 2001). These attributes provide a compelling geochronological connection between the Mount Isa inlier in Australia and the Coal Creek inlier in Yukon, which, if valid, would imply extension and constrain the age of the PR1 basin to <1460 Ma.

Taken together, the Racklan and Isan orogenies provide a history of episodic convergence between northwestern Laurentia and northeastern Australia over an interval of approximately 100 Ma. Eglington et al. (2013) also suggest that these orogenic events were linked, and drove fluid flow through sedimentary basins on Laurentia leading to the development of uranium mineralization in the Athabasca and Thelon basins between ca. 1670 and 1500 Ma. The Racklan orogeny defines closure of an open ocean basin and the obduction of Bonnetia at ca. 1600 Ma (Furlanetto et al., 2013; Nielsen et al., 2013). After a hiatus in deformation, the second phase of the Isan orogeny, from ca. 1540–1500 Ma, records the principal collision between the continents and the amalgamation of Australia into supercontinent Columbia. Northeastern Australia absorbed most of the deformation because it was hotter and weaker, arguably because it was under the influence of both

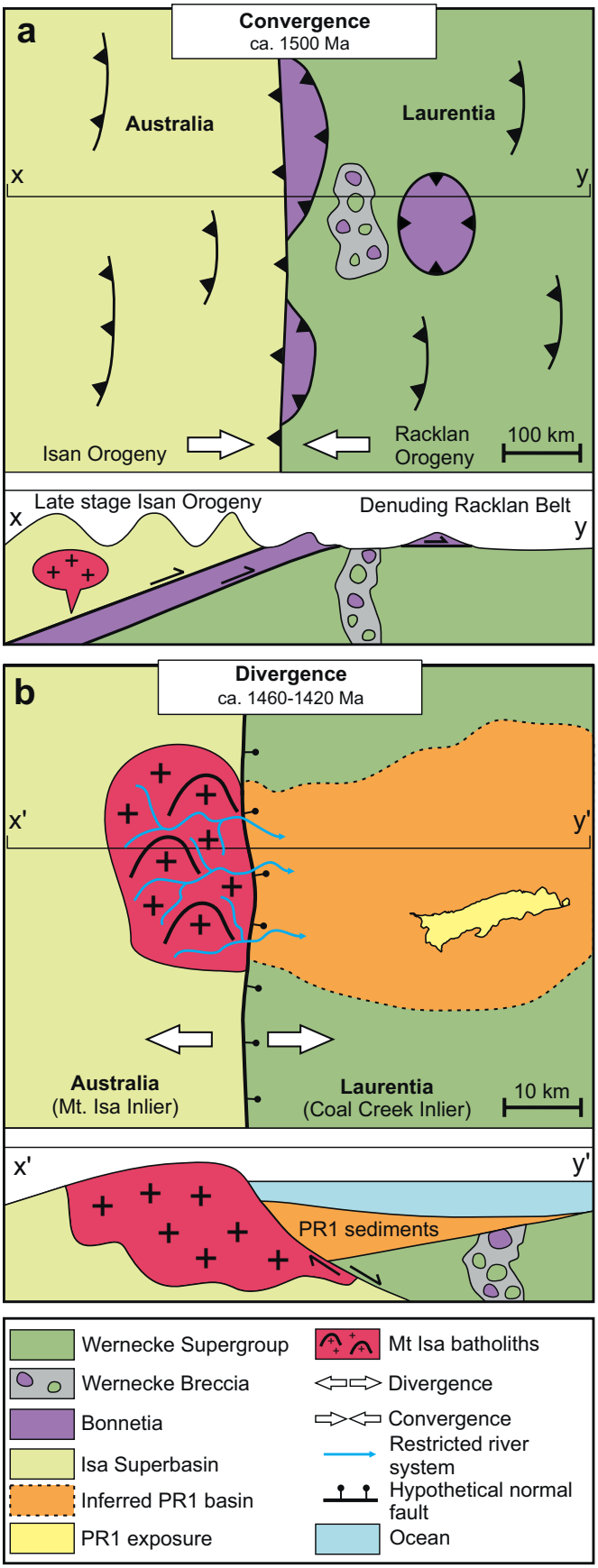

Fig. 10. Plan and cross-sectional views of Australia (Mount Isa inlier) and Laurentia (Coal Creek inlier) during formation and breakup of supercontinent Columbia. (a) Convergence of northeastern Australia and northwestern Laurentia and intrusion of the Williams and Naraku batholiths ca. 1500 Ma. Convergence resulted in the formation of the Racklan and Isan orogens. The Racklan orogen underwent erosion and peneplanation prior to development of the PR1 basin. (b) Beginning of extension of supercontinent Columbia. After exhumation of the Williams and Naraku batholiths (<1460 Ma) a short and restricted river network transported sediment into the PR1 basin.

subduction and a migrating mantle plume (Betts et al., 2009). By 1500 Ma the continents were sutured, and we suggest that the Mount Isa and Coal Creek regions lay adjacent to one another (Fig. 10a). Mountains probably formed on both continents during the Racklan–Isan event, but during the ensuing tens of millions of years this part of Columbia was apparently reduced to a low-lying peneplain (Furlanetto et al., 2013; Nielsen et al., 2013). Subsequent extension led to localized uplift and unroofing of the Williams and Naraku batholiths (<1460 Ma). The exhumed batholiths then formed a local highland adjacent to the newly formed PR1 basin, providing the vast majority of sediment to the basin, with very minor input from other older, and possibly more distal, sources on Laurentia and/or Australia (Fig. 10b).

5.3. Correlation with Basins in the southern Cordillera

The lower Fifteenmile group has previously been correlated with the Pinguicula Group in the Hart River and Wernecke inliers based on lithostratigraphic similarities (Fig. 1b; Abbott, 1997; Medig et al., 2010). The most recent correlations align unit PR1 of the lower Fifteenmile group with units A and B of the Pinguicula Group and unit PR2 of the lower Fifteenmile group with unit C of the Pinguicula Group (Medig et al., 2010). Based on data presented here, the PR1 basin is older than the <1380 Ma Pinguicula basin (Medig et al., 2010), and previous correlations no longer apply. The age of the PR1 basin is unique in Yukon and no other northwestern Laurentian basins have a similar age of deposition. Basins in southwestern Laurentia; however, do have similar ages of deposition as the PR1 basin in Yukon.

We suggest that the Belt-Purcell basin in southeastern British Columbia, Montana, and Idaho, the Hess Canyon basin in Arizona, and the Trampas basin in New Mexico may have been active at the same time as the PR1 basin as they also contain detrital zircon grains with ages that fall into NAMG (Fig. 11; Ross and Villeneuve, 2003; Stewart et al., 2010; Doe et al., 2012; Daniel et al., 2013). The inclusion of NAMG-aged zircon grains suggests that a portion of the sediment from these basins, as with the PR1 basin, is derived from a non-Laurentian source. The majority of NAMG-aged zircon from the Belt-Purcell, Hess Canyon, and Trampas basins are older than those from the PR1 basin, falling into the earlier half of the NAMG (Ross and Villeneuve, 2003; Doe et al., 2012; Daniel et al., 2013). Source areas for these zircon grains plausibly match areas in southern Australia such as the Gawler Craton, the Curnamona Province, and the Musgrave Province/Arunta inlier and areas in the Terre Adélie Craton and the Transantarctic Mountains in Antarctica where granitoid clasts of similar ages were collected (Ross et al., 1992; Peucat et al., 2002; Fanning, 2003; Ross and Villeneuve, 2003; Goodge et al., 2010). Unlike the near-unimodal population from the PR1 basin that requires a proximal and single source, the wider range of NAMG-aged zircon as well as the abundant Paleoproterozoic and Archean grains from the Belt-Purcell, Hess Canyon, and Trampas basins suggests multiple sources from possibly more distal locations. Paleoproterozoic and Archean grains may be derived from either Laurentian or non-Laurentian Paleoproterozoic and Archean sources; however, NAMG-aged grains may only be derived from Australia and Antarctica (Ross et al., 1992; Fanning, 2003; Goodge et al., 2010). The range of sources available to the Belt-Purcell, Hess Canyon, and Trampas basins and the possibility for greater distances travelled allows for variable positioning of Australia with respect to Laurentia. With northeast Australia tightly fit to northwestern Laurentia, it follows that the southern basins would be sourced from southern Australia and Antarctica (Fig. 12).

The proposed timing of extension and formation of the PR1 basin is broadly similar to the opening of rift basins in southwestern Laurentia (Ross and Villeneuve, 2003; Doe et al., 2012; Daniel et al., 2013). The Belt-Purcell, Hess Canyon, and Trampas basins have

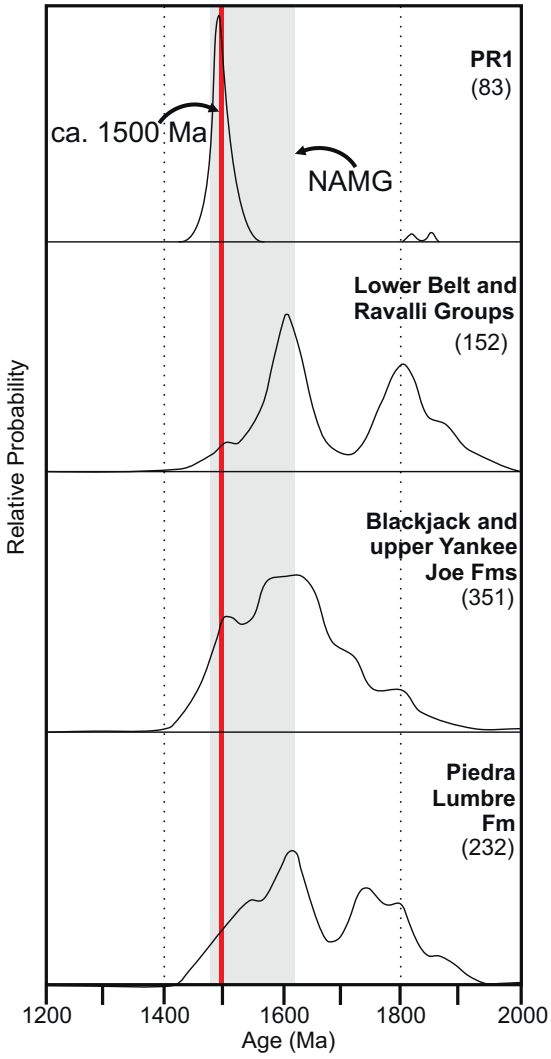

Fig. 11. Probability distribution diagrams comparing NAMG-aged detrital zircon populations (Pb/Pb ages) in four separate basins in the Cordillera (adapted from Doe et al., 2012). Grey interval represents NAMG from 1610 to 1490 Ma. Red interval represents the near-unimodal concordia U/Pb upper intercept age of 1499 Ma. Polymodal data from the Lower Belt and Ravalli Groups from the Belt-Purcell Supergroup, the Blackjack and upper Yankee Joe Formations from the Hess Canyon Group, and the Piedra Lumbre Formation from the Trampas Group.

depositional ages between 1470 and 1401 Ma, 1488 and 1436 Ma, and 1475 and 1450 Ma (Evans et al., 2000; Doe et al., 2012; Daniel et al., 2013), respectively, which are similar to the probable age of the PR1 basin formation as inferred from the timing of exhumation of the proposed source-rocks (1460–1420 Ma). The similarity in ages of the PR1, Belt-Purcell, Hess Canyon, and Trampas basins, suggests that supercontinent Columbia underwent extension, without full continental separation, along a north–south axis that extended for a minimum of 4300 km (Fig. 12).

5.4. Refining continental configurations

Proposed linkages between Laurentia and the amalgam of Antarctica and Australia are based on a range of data types including sedimentary provenance (Ross and Villeneuve, 2003), metallogenesis (Thorkelson et al., 2005), shared igneous belts (Karlstrom et al., 2001; Goodge et al., 2010), shared deformational histories (Karlstrom et al., 2001; Thorkelson et al., 2005; Duebendorfer et al., 2006; Betts et al., 2009), and paleomagnetic compatibility (Pesonen et al., 2012; Pisarevsky et al., 2014). However,

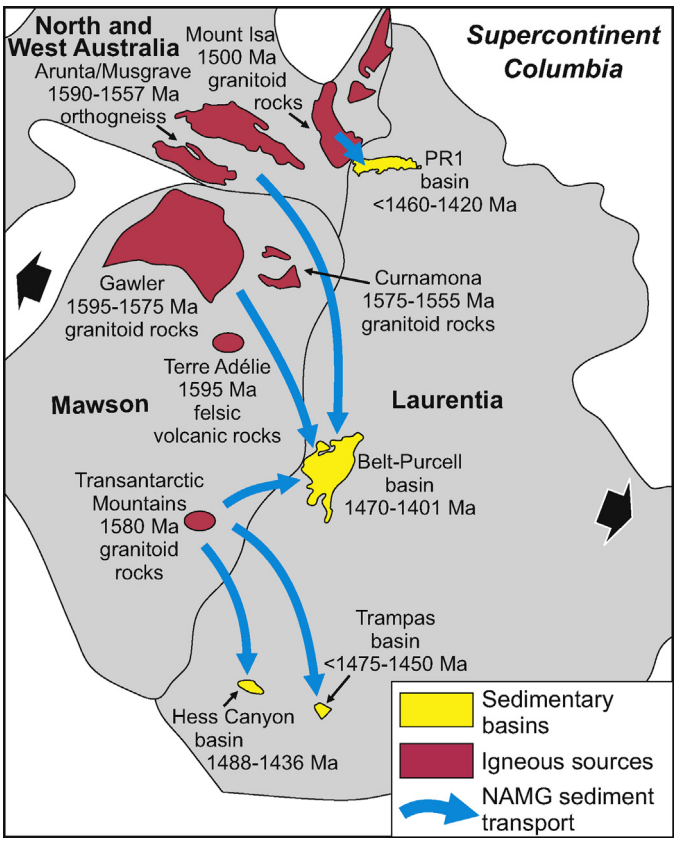

Fig. 12. Configuration of North and West Australia, Laurentia, and Mawson continent (South Australia Gawler Craton and Antarctica) during extension of supercontinent Columbia ca. 1450 Ma. River networks (blue arrows) transport sediment from NAMG-aged igneous sources into sedimentary basins. Red ellipses on Mawson continent depict point sources in East Antarctica and Terre Adélie of unknown extent. Grey polygons represent continents in the Mesoproterozoic (after Payne et al., 2009) and black arrows illustrate extension direction of continents resulting in basin formation. (For interpretation of the references to colour in this figure legend, the reader is referred to the web version of this article.)

the postulated reconstructions that utilize these linkages differ significantly in the latitudinal positions of the continents, with the Mount Isa inlier ranging as far south as present-day central British Columbia (Stewart et al., 2010) or as far north as the present day Arctic Ocean (Payne et al., 2009), a difference of approximately 2000 km. The differences in reconstruction are largely an outcome of weaknesses in the proposed linkages. For example, a provenance linkage between the Belt-Purcell basin and probable source areas in Australia is based on a polymodal detrital zircon population that could reflect a long and complex river system (Ross and Villeneuve, 2003). The concept of a long and complex river network was used by proponents of a Siberia–western Laurentia model (Sears et al., 2004) that placed Siberia north of Australia and adjacent to the Belt-Purcell basin in Laurentia, and brought Australian sediment north across Siberia and east into the Belt-Purcell basin. Given the variability in the proposed length and orientation of the fluvial transport system, the Belt-Purcell provenance linkage is not effective in determining the paleo-position of Australia–East Antarctica relative to Laurentia. Comparable provenance ties involving the Hess Canyon and Trampas basins and Australia (Doe et al., 2012; Daniel et al., 2013) involve a similar degree of uncertainty in continental paleo-position.

6. Conclusion

The PR1 provenance linkage, with its near-unimodal detrital zircon population and inferred short fluvial transport distance from a proximal point source, brings increased resolution to the configuration of Columbia during the early Mesoproterozoic. The Coal Creek inlier in Yukon, Canada was situated directly next to the Mount Isa inlier of northeastern Australia, resulting in a short distance of sediment transport from source to basin. Pinning northeastern Australia to northwestern Laurentia also aligns older NAMG sediment sources from southern Australia and Antarctica to Mesoproterozoic basins along the southwestern Laurentian margin. This paleogeographic outcome is nearly identical to the SWEAT configuration used for the younger supercontinent Rodinia (Moores, 1991) and does not permit Siberia or China to lie adjacent to western Laurentia in the early Mesoproterozoic. It follows that the configuration of this part of Columbia remained fundamentally intact for at least 200 m.y., starting with the convergence of Australia and Laurentia from 1600 to 1500 Ma, continuing with the extension of Columbia beginning around 1490 Ma to form basins such as the PR1, Belt-Purcell, Hess Canyon, and Trampas, and disassembling in the middle to late Mesoproterozoic (Pisarevsky et al., 2014). How a Mesoproterozoic break-up of western Columbia should be reconciled with the proposed juncture of Australia–Antarctica–Laurentia in Rodinia (Moores, 1991; Karlstrom et al., 1999; Li et al., 2008) remains unresolved.

Acknowledgements

Funding for the project was provided by the Yukon Geological Survey, the Geological Survey of Canada, Northern Scientific Training Program, and an NSERC grant to Derek Thorkelson. Tom Pestaj is thanked for his assistance at the SHRIMP laboratory and Pat Hunt for SEM imaging. John Lydon is thanked for valuable suggestions that improved the manuscript. Jaap Verbaas and Robbie Dunlop are thanked for their assistance in the field. Two anonymous reviewers significantly improved the manuscript.

Appendix A. Supplementary data

Supplementary material related to this article can be found, in the online version, at http://dx.doi.org/10.1016/j.precamres.2014.04.018.

References

Abbott, G., 1997. Geology of the upper Hart River area, eastern Ogilvie Mountains, Yukon Territory (116A/10,116 A/11). Exploration and Geological Services Division, Yukon, Indian and Northern Affairs Canada. Bulletin 9, 1–92.
Betts, P., Giles, D., 2006. The 1800–1100 Ma tectonic evolution of Australia. Precambrian Res. 144, 92–125.
Betts, P., Giles, D., Schaefer, B., 2008. Comparing 1800–1600 Ma accretionary and basin processes in Australia and Laurentia: possible geographic connections in Columbia. Precambrian Res. 166, 81–92.
Betts, P.G., Giles, D., Foden, J., Schaefer, B.F., Mark, G., Pankhurst, M.J., Forbes, C.J., Williams, H.A., Chalmers, N.C., Hills, Q., 2009. Mesoproterozoic plume-modified orogenesis in eastern Precambrian Australia. Tectonics 28, 1–28.
Brideau, M.-A., Thorkelson, D.J., Godin, L., Laughton, J.R., 2002. Paleoproterozoic deformation of the Racklan Orogeny, Slats Creek (106D/16) and Fairchild Lake (106C/13) map areas, Wernecke Mountains, Yukon. In: Emond, D.S., Weston, L.H., Lewis, L.L. (Eds.), Yukon Exploration and Geology. Exploration and Geological Services Division, Yukon Region, Indian and Northern Affairs Canada, pp. 65–72.
Buchan, K.L., 2013. Key paleomagnetic poles and their use in Proterozoic continent and supercontinent reconstructions: a review. Precambrian Res. 238, 93–110.
Cawood, P.A., Nemchin, A.A., Freeman, M., Sircombe, K., 2003. Linking source and sedimentary basin: detrital zircon record of sediment flux along a modern river system and implications for provenance studies. Earth Planet. Sci. Lett. 210, 259–268.
Chamberlain, K.R., Schmitt, A.K., Swapp, S.M., Harrison, T.M., Swoboda-Colberg, N., Bleeker, W., Peterson, T.D., Jefferson, C.W., Khudoley, A.K., 2010. In situ U–Pb SIMS (IN-SIMS) micro-baddeleyite dating of mafic rocks: method with examples. Precambrian Res. 183, 379–387.
Condie, K.C., Belousova, E., Griffin, W.L., Sircombe, K.N., 2009. Granitoid events in space and time: constraints from igneous and detrital zircon age spectra. Gondwana Res. 15, 228–242.

Daniel, C.G., Pfeifer, L.S., Jones, J.V., 2013. Detrital zircon evidence for non-Laurentian provenance, Mesoproterozoic (ca. 1490–1450 Ma) deposition and orogenesis in a reconstructed orogenic belt, northern New Mexico, USA: defining the *Picuris orogeny*. Geol. Soc. Am. Bull. 125, 1423–1441.

Doe, M.F., Jones, J.V., Karlstrom, K.E., Thrane, K., Frei, D., Gehrels, G., Pecha, M., 2012. Basin formation near the end of the 1.60–1.45 Ga tectonic gap in southern Laurentia: Mesoproterozoic Hess Canyon Group of Arizona and implications for ca. 1.5 Ga supercontinent configurations. Lithosphere 4, 77–88.

Doughty, P.T., Price, R.A., Parrish, R.R., 1998. Geology and U–Pb geochronology of Archean basement and Proterozoic cover in the Priest River complex, northwestern United States, and their implications for Cordilleran structure and Precambrian continent reconstructions. Can. J. Earth Sci. 35, 39–54.

Duebendorfer, E.M., Chamberlain, K.R., Heizler, M.T., 2006. Filling the North American Proterozoic tectonic gap: 1.60–1.59-Ga deformation and orogenesis in southern Wyoming, USA. J. Geol. 114, 19–42.

Eglington, B.M., Pehrsson, S.J., Ansdell, K.M., Lescuyer, J.L., Quirt, D., Milesi, J.P., Brown, P., 2013. A domain-based digital summary of the evolution of the Palaeoproterozoic of North America and Greenland and associated unconformity-related uranium mineralization. Precambrian Res. 232, 4–26.

Ernst, R.E., Buchan, K.L., Hamilton, M.A., Okrugin, A.V., Tomshin, M.D., 2000. Integrated paleomagnetism and U–Pb geochronology of mafic dikes of the Eastern Anabar Shield Region, Siberia: implications for mesoproterozoic paleolatitude of Siberia and comparison with Laurentia. J. Geol. 108, 381–401.

Ernst, R.E., Pereira, E., Hamilton, M.A., Pisarevsky, S.A., Rodriques, J., Tassinari, C.C., Teixeira, W., Van-Dunem, V., 2013. Mesoproterozoic intraplate magmatic "barcode"record of the Angola portion of the Congo craton: newly dated magmatic events at 1500 and 1110 Ma and implications for Nuna (Columbia) supercontinent reconstructions. Precambrian Res. 230, 103–118.

Evans, D.A., Mitchell, R.N., 2011. Assembly and breakup of the core of paleoproterozoic–mesoproterozoic supercontinent Nuna. Geology 39, 443–446.

Evans, K.V., Aleinikoff, J.N., Obradovich, J.D., Fanning, C.M., 2000. SHRIMP U–Pb geochronology of volcanic rocks, Belt Supergroup, western Montana: evidence for rapid deposition of sedimentary strata. Can. J. Earth Sci. 37, 1287–1300.

Fanning, C.M., 2003. Detrital zircon provenance of the Mesoproterozoic Pandurra Formation, South Australia: Gawler Craton zircon population and implications for the Belt Supergroup. In: Presented at the 2003 GSA Annual Meeting, Seattle.

Furlanetto, F., Thorkelson, D.J., Daniel, G.H., Marshall, D.D., Rainbird, R.H., Davis, W.J., Crowley, J.L., Vervoort, J.D., 2013. Late Paleoproterozoic terrane accretion in northwestern Canada and the case for circum-Columbian orogenesis. Precambrian Res. 224, 512–528.

Goodge, J.W., Fanning, C.M., Brecke, D.M., Licht, K.J., Palmer, E.F., 2010. Continuation of the Laurentian Grenville Province across the Ross Sea Margin of East Antarctica. J. Geol. 118, 601–619.

Hamilton, M.A., Buchan, K.L., 2010. U–Pb geochronology of the Western Channel Diabase, northwestern Laurentia: implications for a large 1.59 Ga magmatic province, Laurentia's APWP and paleocontinental reconstructions of Laurentia, Baltica and Gawler craton of southern Australia. Precambrian Res. 183, 463–473.

Heaman, L.M., Gower, C.F., Perreault, S., 2004. The timing of Proterozoic magmatism in the *Pinware terrane* of southeast Labrador, easternmost Quebec and northwest Newfoundland. Can. J. Earth Sci. 41, 127–150.

Hou, G., Santosh, M., Qian, X., Lister, G., Li, J., 2008. Configuration of the Late Paleoproterozoic supercontinent Columbia: insights from radiating mafic dyke swarms. Gondwana Res. 14, 395–409.

Karlstrom, K.E., Åhäll, K.-I., Harlan, S.S., Williams, M.L., McLelland, J., Geissman, J.W., 2001. Long-lived (1.8–1.0 Ga) convergent orogen in southern Laurentia, its extensions to Australia and Baltica, and implications for refining Rodinia. Precambrian Res. 111, 5–30.

Karlstrom, K.E., Harlan, S., Williams, M., McLelland, J., Geissman, J.W., Ahall, K.I., 1999. Refining Rodinia: geologic evidence for the Australia–western US connection in the Proterozoic. GSA Today 9, 1–7.

Li, Z.X., Bogdanova, S.V., Collins, A.S., Davidson, A., De Waele, B., Ernst, R.E., Fitzsimons, I.C.W., Fuck, R.A., Gladkochub, D.P., Jacobs, J., Karlstrom, K.E., Lu, S., Natapov, L.M., Pease, V., Pisarevsky, S.A., Thrane, K., Vernikovsky, V., 2008. Assembly, configuration, and break-up history of Rodinia: a synthesis. Precambrian Res. 160, 179–210.

Ludwig, K., 2009. SQUID 2: A User's Manual. In: Berkeley Geochronology Center Special Publication No. 5. Berkeley Geochronology Center, Berkeley, pp. 1 (rev. 12 April 2009).

Ludwig, K., 2012. User's Manual for Isoplot 3.75. In: Berkeley Geochronology Center Special Publication No. 5. Berkeley Geochronology Center, Berkeley, pp. 1.

Macdonald, F., Schmitz, M., Crowley, J., Roots, C., Jones, D., Maloof, A., Strauss, J., Cohen, P., Johnston, D., Schrag, D., 2010. Calibrating the cryogenian. Science 327, 1241–1243.

MacLean, B., Cook, D., 2004. Revisions to the Paleoproterozoic sequence A, based on reflection seismic data across the western plains of the Northwest Territories, Canada. Precambrian Res. 129, 271–289.

Medig, K.P.R., Thorkelson, D.J., Dunlop, R.L., 2010. The Proterozoic Pinguicula Group: stratigraphy, contact relationships, and possible correlations. In: Yukon Exploration and Geology 2009. Yukon Geological Survey, pp. 265–278.

Meert, J.G., 2002. Paleomagnetic evidence for a Paleo-Mesoproterozoic supercontinent Columbia. Gondwana Res. 5, 207–215.

Meert, J.G., 2012. What's in a name? The Columbia (Paleopangaea/Nuna) supercontinent. Gondwana Res. 21, 987–993.

Moores, E.M., 1991. Southwest US–East Antarctic (SWEAT) connection: a hypothesis. Geology 19, 425–428.

Nielsen, A.B., Thorkelson, D.J., Gibson, H.D., 2013. The Wernecke igneous clasts in Yukon, Canada: fragments of the Paleoproterozoic volcanic arc terrane Bonnetia. Precambrian Res. 238, 78–92.

Page, R.W., Sun, S.S., 1998. Aspects of geochronology and crustal evolution in the Eastern Fold Belt, Mt Isa Inlier. Aust. J. Earth Sci. 45, 343–361.

Payne, J.L., Hand, M., Barovich, K.M., Reid, A., Evans, D.A.D., 2009. Correlations and Reconstruction Models for the 2500–1500 Ma Evolution of the Mawson Continent. Geological Society London Special Publications, 323. Geological Society, London, pp. 319.

Pehrsson, S.J., Berman, R.G., Eglington, B., Rainbird, R., 2013. Two Neoarchean supercontinents revisited: the case for a Rae family of cratons. Precambrian Res. 232, 27–43.

Pesonen, L.J., Mertanen, S., Veikkolainen, T., Ndougsa-Mbarga, T., Feumoe, A.N.S., Manguelle-Dicoum, E., Fairhead, J.D., 2012. Paleo-Mesoproterozoic supercontinenta paleomagnetic view. Geophysica 48, 5–47.

Peucat, J.J., Capdevila, R., Fanning, C.M., Ménot, R.P., Pécora, L., Testut, L., 2002. 1.60 Ga felsic volcanic blocks in the moraines of the Terre Adélie Craton, Antarctica: comparisons with the Gawler Range Volcanics, South Australia. Aust. J. Earth Sci. 49, 831–845.

Pisarevsky, S.A., Elming, S.-Å., Pesonen, L.J., Li, Z.-X., 2014. Mesoproterozoic paleogeography: supercontinent and beyond. Precambrian Res. 244, 207–225.

Rainbird, R., McNicoll, V., Theriault, R., Heaman, L., Abbott, J., Long, D., Thorkelson, D., 1997. Pan-continental river system draining Grenville orogen recorded by U–Pb and Sm–Nd geochronology of Neoproterozoic quartzarenites and mudrocks, northwestern Canada. J. Geol. 105, 1–17.

Rogers, J., Santosh, M., 2002. Configuration of Columbia, a Mesoproterozoic supercontinent. Gondwana Res. 5, 5–22.

Ross, G., Villeneuve, M., 2003. Provenance of the Mesoproterozoic (1.45 Ga) Belt basin (western North America): another piece in the pre-Rodinia paleogeographic puzzle. Geol. Soc. Am. Bull. 115, 1191–1217.

Ross, G.M., Parrish, R.R., Winston, D., 1992. Provenance and U–Pb geochronology of the Mesoproterozoic Belt Supergroup (northwestern United States): implications for age of deposition and pre-Panthalassa plate reconstructions. Earth Planet. Sci. Lett. 113, 57–76.

Sears, J., Price, R., 2002. The hypothetical Mesoproterozoic supercontinent Columbia: implications of the Siberian-west Laurentian connection. Gondwana Res. 5, 35–39.

Sears, J., Price, R., Khudoley, A., 2004. Linking the Mesoproterozoic Belt-Purcell and Udzha basins across the west Laurentia–Siberia connection. Precambrian Res. 129, 291–308.

Silveira, E.M., Söderlund, U., Oliveira, E.P., Ernst, R.E., Leal, A.B., 2013. First precise U–Pb baddeleyite ages of 1500 Ma mafic dykes from the São Francisco Craton, Brazil, and tectonic implications. Lithos 174, 144–156.

Sláma, J., Košler, J., 2012. Effects of sampling and mineral separation on accuracy of detrital zircon studies. In: Geochemistry Geophysics Geosystems., pp. 13.

Spikings, R.A., Foster, D.A., Kohn, B.P., Lister, G.S., 2001. Post-orogenic (<1500 Ma) thermal history of the Proterozoic Eastern Fold Belt, Mount Isa Inlier, Australia. Precambrian Res. 109, 103–144.

Stern, R., 1997. The GSC sensitive high resolution ion microprobe (SHRIMP): analytical techniques of zircon U–Th–Pb age determinations and performance evaluation. In: Radiogenic Age and Isotopic Studies: Report 10. Current Research 1997-F. Geological Survey of Canada, pp. 1–31.

Stern, R., Amelin, Y., 2003. Assessment of errors in SIMS zircon U–Pb geochronology using a natural zircon standard and NIST SRM 610 glass. Chem. Geol. 197, 111–142.

Stewart, E.D., Link, P.K., Fanning, C.M., Frost, C.D., McCurry, M., 2010. Paleogeographic implications of non-North American sediment in the Mesoproterozoic upper Belt Supergroup and Lemhi Group, Idaho and Montana, USA. Geology 38, 927–930.

Thompson, R.I., Roots, C.F., Mustard, P.S., 1992. Geology of Dawson Map Area (116B,C) (northeast of Tintina Trench). Geological Survey of Canada, Canada.

Thorkelson, D.J., Abbott, J.G., Mortensen, J.K., Creaser, R.A., Villeneuve, M.E., McNicoll, V.J., Layer, P.W., 2005. Early and middle Proterozoic evolution of Yukon, Canada. Can. J. Earth Sci. 42, 1045–1071.

Torsvik, T.H., 2003. The Rodinia jigsaw puzzle. Science 300, 1379–1381.

Vermeesch, P., 2004. How many grains are needed for a provenance study? Earth Planet. Sci. Lett. 224, 441–451.

Zhao, G., Cawood, P., Wilde, S., Sun, M., 2002. Review of global 2.1–1.8 Ga orogens: implications for a pre-Rodinia supercontinent. Earth Sci. Rev. 59, 125–162.